Assimilation of satellite reflectance data into a dynamical leaf model to infer seasonally varying leaf areas for climate and carbon models

Q. Liu,[1] L. Gu,[2] R. E. Dickinson,[1] Y. Tian,[3] L. Zhou,[1] and W. M. Post[2]

[1] Leaf area index is an important input for many climate and carbon models. The widely used leaf area products derived from satellite-observed surface reflectances contain substantial erratic fluctuations in time due to inadequate atmospheric corrections and observational and retrieval uncertainties. These fluctuations are inconsistent with the seasonal dynamics of leaf area, known to be gradual. Their use in process-based terrestrial carbon models corrupts model behavior, making diagnosis of model performance difficult. We propose a data assimilation approach that combines the satellite observations of Moderate Resolution Imaging Spectroradiometer (MODIS) albedo with a dynamical leaf model. Its novelty is that the seasonal cycle of the directly retrieved leaf areas is smooth and consistent with both observations and current understandings of processes controlling leaf area dynamics. The approach optimizes the dynamical model parameters such that the difference between the estimated surface reflectances based on the modeled leaf area and those of satellite observations is minimized. We demonstrate the usefulness and advantage of our new approach at multiple deciduous forest sites in the United States.

1. Introduction

[2] The leaf area index (LAI), defined as the one-sided leaf area per unit ground surface area is a major land surface parameter. Its seasonal dynamics has a strong influence on the variation of mass and energy exchanges between the surface and the atmosphere. The performance of land surface models depend on how well the seasonal dynamics of LAI is represented, either internally or using observations as input. It is difficult to predict LAI internally in land surface models because biological and environmental processes affecting LAI are numerous and often not well understood. For this reason, most land surface models now use remote sensing products of LAI as input [*Zeng et al.*, 2002; *Tian et al.*, 2004]. Satellite-observed spectral surface reflectances are now routinely used to generate LAI products [e.g., *Myneni et al.*, 2002; *Lotsch et al.*, 2003], products that are now indispensable for study of climate change and terrestrial responses.

[3] Satellite observations are affected by atmospheric composition, clouds and aerosols, and other dynamic fac-tors. Consequently, the LAI derived from satellite surface reflectance observations often contain large, erratic fluctuations while the actual temporal variation in LAI would be more gradual and smooth. For land surface modeling and particularly carbon cycle modeling, such erratic fluctuations are not simply a noise issue; they lead to a series of problems in predicted carbon budgets and energy fluxes. For instance, when LAI increases, the carbon and nutrients needed for this increased LAI must be accounted for to maintain mass conservation and consistency among different carbon and nutrient pools in the model. Growth and maintenance respiration must also increase accordingly. An LAI with large temporal discontinuities will shift growth respiration unreasonably, and introduce problematical imbalance between carbon and nutrients. Erratic fluctuations in LAI products can also cause problems in their application for studies in phenology. Therefore, a resolution of the issue of erratic fluctuations would enhance the value of remote sensing–based LAI products for climate change research.

[4] Efforts to reduce erratic fluctuations in satellite LAI products have mostly focused on advancing the algorithm of the retrieval process for surface radiative fluxes that are used for LAI estimation [e.g., *Bicheron and Leroy*, 1999; *Yang et al.*, 2006; *Deng et al.*, 2006], or using statistical procedures to smooth erratic fluctuations after the LAI products are generated [e.g., *Chen et al.*, 2002; *Roerink et al.*, 2000; *Chen et al.*, 2006]. While these approaches are valuable, their effectiveness is ultimately limited by the dynamics of the atmosphere and by the quality of upstream data sets that enable the calculation of LAI. An alternative

[1]School of Earth and Atmospheric Sciences, Georgia Institute of Technology, Atlanta, Georgia, USA.
[2]Environmental Sciences Division, Oak Ridge National Laboratory, Oak Ridge, Tennessee, USA.
[3]Center for Satellite Applications and Research, IMSG, National Environmental Satellite Data and Information Service, NOAA, Camp Springs, Maryland, USA.
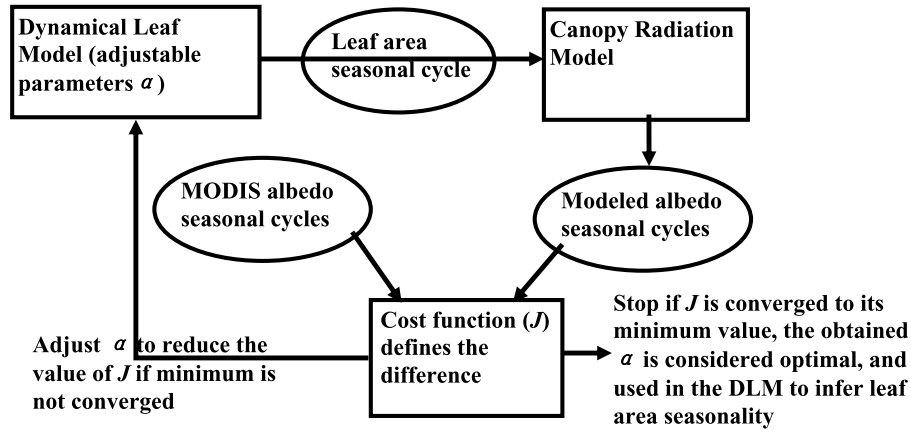
Figure 1. Schematic overview of the proposed data assimilation approach.

approach proposed here is to constrain the estimates of LAI by combining our understanding of the dynamics of canopy processes with MODIS observations of surface albedo through data assimilation. Although MODIS LAI products can be used for similar purposes, their errors resulted from processing the MODIS reflectance data are bigger and more difficult to quantify than those of the MODIS albedo products. The proposed approach adds additional information in the form of a priori ecological knowledge to enhance the remote sensing algorithms. Furthermore, it applies to the very process of LAI estimation, in contrast to a preprocessing strategy [e.g., *Deng et al.*, 2006] or a postprocessing strategy [e.g., *Chen et al.*, 2006].

[5] This article details our approach and tests it at multiple sites.

2. Methods

2.1. Overall Strategy

[6] In current remote sensing, each set of measurement inverted for leaf area is viewed as an independent estimate. However, leaf areas at different times are inherently linked through plant growth and developmental processes. As a result, the LAI products as currently derived are contaminated by large errors in the upstream products of surface reflectance and by uncertainties in the algorithm that infers LAI from surface reflectance.

[7] A recently developed dynamic leaf model (DLM) [*Dickinson et al.*, 2008] makes it possible to use the inherent, biological linkage in the temporal variations of leaf area to improve the quality of remote sensing products of LAI. This DLM uses a minimum number of vegetation-specific parameters to describe the influences of environmental variations on the temporal evolution of LAI and thus is particularly suitable for large-scale applications. Our strategy is straightforward: we optimize the parameters in the DLM by minimizing the difference between satellite-based surface albedos and the albedos calculated with a canopy radiative transfer model that uses the temporal dynamics of LAI predicted by the DLM. The process is iterative and once the optimization process is completed, the temporal dynamics of LAI are produced by the DLM with the optimized set of parameters.

[8] In addition to satellite observations of surface albedos and the DLM, our data assimilation system requires a third component, that is, a canopy radiative transfer model to link LAI with surface albedos. For this purpose, we use a two-stream radiative transfer scheme [e.g., *Dickinson*, 1983; *Sellers et al.*, 1986; *Pinty et al.*, 2006]. Such a two stream model has been widely used in climate models, although more complicated schemes are available [e.g., *Schaaf et al.*, 2002; *Myneni et al.*, 2002; *Knyazikhin et al.*, 1998a, 1998b] that might be similarly used.

[9] A schematic overview of the proposed data assimilation approach is illustrated in Figure 1. To evaluate the performance of our approach, we also conduct a direct inversion of the LAI using the canopy radiation model alone, and compare the LAI seasonal cycle of the optimized DLM simulations with that of the direct inversion, and the MODIS products.

2.2. Dynamical Leaf Model

[10] The DLM [*Dickinson et al.*, 2008] simulates the seasonal leaf area dynamics on a daily time step. The most important short-term drivers of natural canopy variability are thermal and water stresses, and so only temperature and soil moisture are included as forcing input to the model, and for a cold weather deciduous forest, the temperature stress is dominant. The DLM gives dynamics of leaf area (L) as

$$\frac{dL}{dt} = -\lambda(L, \boldsymbol{\alpha}, T) \cdot L, \tag{1}$$

where the term λ is the inverse of the timescale over which L grows (negative) or decays (positive), $\boldsymbol{\alpha}$ is a vector of all parameters, T is air temperature, which is the only atmospheric forcing here. The term λ is formulated as

$$\lambda = \lambda_0\{1 + a[1 - R(x)]\} - \lambda_0\left\{R(x)\left(\frac{L_0}{L}\right)\left[1 - e^{-cL}\right]\right\}. \tag{2}$$

The two portions on the right are the stress and gain terms, respectively. The parameter λ_0 is an inverse timescale characterizing normal respiration losses balancing at steady state normal growth. In the stress term, a expresses enhanced loss from stress terms, $R(x)$ is a smooth Heaviside

"ramp-up" function going from 0 at large negative x values to 1 at large positive x values for which we assume that $R(x) = 0.5(1 + \tanh(x)) = 1/(1 + \exp(-2x))$. The term x is the temperature normalized to the range of temperatures over which cold stress switches off, given as $x = (T - T_{min})/\Delta T$. The growth term describes the light-dependent physiology, in which L_0 is the maximum leaf area possible under light limit, c is a parameter determining the dependence of L on light attenuation. In order to push L away from its unstable equilibrium point $L = 0$, the value of L is limited to no less than 0.1, representing a small "photosynthate" storage term in winter. The above formulation requires a total of six parameters, T_{min}, ΔT, λ_0, L_0, a, c. In our study, we found that the parameters a and c, inferred from data fitting, have strong correlation. Therefore, we assumed c at a fixed value of 1. Thus, only five parameters are adjusted by the data assimilation, i.e., the adjustable vector $\alpha = \{T_{min}, \Delta T, \lambda_0, L_0, a\}$.

2.3. Two-Stream Canopy Radiation Model

[11] The numerical code of the two-stream scheme for computing the canopy radiations in this study follows that for radiation fluxes associated with diffuse radiation in *Pinty et al.* [2006]. The formulation details can be found in the work of *Pinty et al.* [2006, equation (33), Appendix B]. The radiation model uses a given LAI to compute the surface albedo, defined as the ratio of upwelling to the spectrally integrated downwelling radiant fluxes at the top of the canopy. Its albedos for visible and near-infrared diffuse radiations are compared with MODIS white-sky albedos. Optical properties, including leaf reflectances, leaf transmittances and soil reflectances for visible and near infrared bands, are prescribed for each site. The leaf reflectance in the near-infrared band is prescribed with values varying with time because we found that a constant value cannot explain the sharp decrease of MODIS albedos in the near-infrared during later half of the growing season in contrast to the smooth pattern of MODIS albedo in the visible band. *Zarco-Tejada et al.* [2003] show how the leaf-level reflectance in the near-infrared spectral region is strongly associated with leaf dry matter weight, water thickness, etc., and older leaves with higher dry matter content have smaller reflectance. Thus, we assume decreasing near-infrared leaf reflectance values for the later half of the growing season. Other optical parameters are assumed constant for simplicity, although they may also vary with time. Their values for a specific site are provided in the following sections.

2.4. Cost Function and Its Minimization

[12] The DLM and MODIS observations are combined through the definition of the cost function. The minimization of the cost function (J) results in the optimal parameter values. The cost functions are based on a widely used least square form, that is,

$$J(\alpha) = \frac{1}{2}\left[(M(\alpha) - O)^T C_o^{-1} (M(\alpha) - O)\right], \qquad (3)$$

where α is the vector of adjustable parameters; O and M contain the observations and their model-simulated counterparts respectively, C_o the associated observational covariance matrix. The proposed approach assimilates MODIS band 1 and band 2 albedos from the linked DLM and

canopy radiation model over a whole year at once to obtain the optimal values of the adjustable DLM parameters, i.e., $\{T_{min}, \Delta T, \lambda_0, L_0, a\}$. Therefore, the observation vector $O = [r_1(t_1)\ r_2(t_1)\ r_1(t_2)\ r_2(t_2)\ \ldots\ r_1(t_n)\ r_2(t_n)]$, where $t_1 \ldots t_n$ are the n MODIS observational time points in the year, r_1 and r_2 are the MODIS albedos in visible band and near infrared band respectively; and the M vector contains the modeled albedos in both band at the same time points. With the assumption of independence between observational points, the $2n \times 2n$ matrix C_o consists of $\sigma_1(t_1)$, $\sigma_2(t_1)$, $\sigma_1(t_2)$, $\sigma_2(t_2)$, ..., $\sigma_1(t_n)$, $\sigma_2(t_n)$ in the diagonal components, and zeros in the nondiagonal components.

[13] Minimization of the cost function is done with a gradient descent search algorithm, requiring both $J(\alpha)$ and its gradient $\nabla J(\alpha)$ with respect to α. The exact evaluation of this gradient can be achieved via the adjoint model of J which is constructed using the automatic differentiation software, TAPENADE [*Hascoët and Pascual*, 2004], and is validated each time with a finite difference approach. The gradient search followed the limited-memory quasi-Newton method developed by *Byrd et al.* [1995] and *Zhu et al.* [1997] for its treatment of bound-constraint conditions. The whole data assimilation process of the new approach is referred to as "dynamical inversion."

[14] For comparison purposes, we also conducted a different type of LAI retrieval experiment from the MODIS albedos: a direct retrieval that assumes LAI at different times of a year as independent variables, and thus uses only the canopy radiation model. It is referred to as "direct inversion," and is done independently at each observational time. The cost function was minimized with respect to the LAI only. The same minimization method and automatic differentiation software as mentioned earlier were applied for the direct inversion. The vector O at a specific time contains two elements: the MODIS observation of visible albedo and near infrared albedo at that point. M contains the corresponding albedos from the canopy radiation model computation. The measurement covariance matrix C_o is assumed diagonal, so that only the variances (σ) have nonzero values. Thus, the cost function for the direct inversion is simplified to

$$J(\text{LAI}) = \sum_{i=1}^{2} \frac{1}{2\sigma_i}(mr_i(\text{LAI}) - or_i)^2, \qquad (4)$$

where the subscript 1 indicates the visible band and 2 the near infrared band, mr and or are the modeled and observed albedos, respectively. The seasonal cycle of the LAI is constructed by repeating the minimization procedure on all observational points collected over the course of a year.

3. Testing Data Sets and Construction of Variances

[15] We tested the new approach described above for observations from three U.S. MODIS validation sites: the Harvard Forest Main Tower (Harvard Forest) in eastern Massachusetts (42°32′N, 72°10′W), the Walker Branch Watershed (Walker Branch) in central Tennessee (35°57′N, 84°17′W), and the Allegheny National Forest (Allegheny) located in northern Pennsylvania (41°52′N, 78°55′W). These sites have relatively uniformly surface
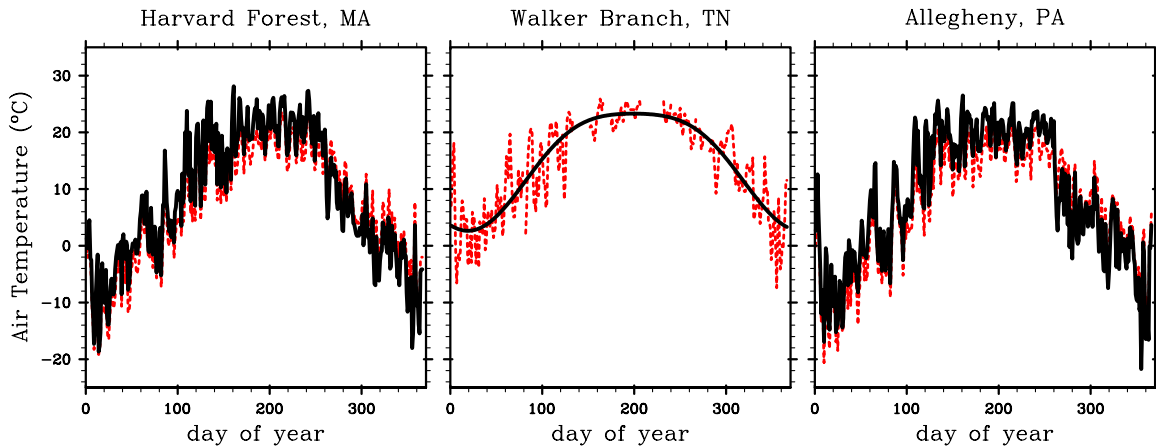
Figure 2. Daily mean of air temperature observations (dashed lines) and the actual time series used (solid lines) to force the dynamic leaf model (DLM) for each site. Harvard Forest and Allegheny use mean daily temperature plus 1 standard deviation before day 140, mean minus 1 standard deviation after day 260, and the mean values in between. Walker Branch uses a fitted second-order Fourier curve to bridge the significant amount of missing points.

coverage of deciduous broadleaf forest. Their MODIS pixel values of land products for a 7×7 km area subsets in ASCII format are archived at the ORNL DAAC data center available through http://www.daac.ornl.gov. We used the MODIS collection 4 16-day, 1-km surface product of Bidirectional Reflectance Distribution Function (BRDF)/Albedo Model parameters (MOD43B1) for the MODIS bands 1 and 2 to compute the white-sky albedos in the visible and near infrared band, respectively, for each pixel. The mean and variance of the 49 pixel values at each time point were taken as the site-level albedos and their observational errors, respectively (shown in Figure 4). The testing time period is year 2004 for the three sites because of overall good data availability. We also used the MODIS collection 4 LAI product (MOD15A2) for comparison. Their site level statistics were computed similarly from pixel values as was done for the albedos.

[16] The site-specific 2004 daily air temperature forcing time series were compiled either from on-site half-hourly flux tower measurement (e.g., Harvard Forest and Walker Branch) or from a nearby weather station hourly measurement when on-site data are unavailable (e.g., Allegheny). The forcing time series for Harvard Forest and Allegheny used mean daily air temperature plus 1 standard deviation of the 48 half-hourly or 24 hourly daily samples before day 140 of the year, mean daily values from day 140 to day 260, and mean daily values minus 1 daily standard deviation after day 260 as it is plausible that daily maximum temperatures are needed for leaf growth in spring and daily minimum values for senescence or frost damage in the fall [*Dickinson et al.*, 2008]. Because the Walker Branch measurement contains a significant amount of missing points (i.e., a total of about 56 days), we used a second-order Fourier curve to fit the valid data points and to create a continuous time series. The fitting artificially smoothed the day-to-day fluctuations of the observations but should have little influence on the seasonal variations of the air temperature. Figure 2 illustrates the actual air temperature measurements and the daily time series used to force the DLM for each site.

[17] The leaf and soil optical properties needed for the canopy radiation model are generally based on the values of broadleaf deciduous forest used in the NCAR Community Land Model [*Oleson et al.*, 2004], and are tuned recursively for each specific site so that the simulated albedo results after data assimilation best agree with the MODIS albedos. Once these values are decided, they are used in both direct and dynamical inversion experiments without further adjustment. Table 1 lists the prescribed optical properties. The leaf reflectance in near infrared shown is the value before day 180 of the year. After day 180, a decrease by 0.001 per day for Walker Branch and Allegheny, and 0.0008 for Harvard Forest is assumed to account for the assumed change of leaf biological properties.

[18] The default values of the dynamical leaf model parameters and their meaningful value ranges are listed in Table 2. The default values were randomly selected from their associated value ranges as they were also used as the initial guess of the control variables for the dynamical inversion for all sites. The value ranges of the DLM parameters were according to the parameter analysis as given by *Dickinson et al.* [2008].

4. Results

[19] Figure 3 shows the LAI seasonal cycle that results from dynamical inversion versus direct inversion, and

Table 1. Values of the Canopy Radiation Model Parameters Used for Each Site[a]

Parameters	Harvard	Walker Branch	Allegheny
Leaf reflectance (vis)	0.06	0.08	0.06
Leaf transmittance (vis)	0.06	0.05	0.05
Soil reflectance (vis)	0.05	0.07	0.07
Leaf reflectance (nir)	0.5	0.5	0.5
Leaf transmittance (nir)	0.40	0.35	0.40
Soil reflectance (nir)	0.21	0.18	0.10

[a]Abbreviations are as follows: vis, visible band; nir, near-infrared band.

Table 2. List of the Parameters Required by the Dynamic Leaf Model[a]

Symbol	Range	Default Values	Harvard Derived	Walker Branch Derived	Allegheny Derived
T_{min} (K)	$273-283$	278	280.4	282.6	277.4
ΔT (K)	$2-8$	5	6.49	7.9	3.16
λ_0	$0.02-0.1$	0.04	0.066	0.1	0.035
L_0	$2-8$	5	8	8	6.308
a	$2-12$	9	5.0	12.0	12.0

[a]Value ranges and default values were predefined. The derived values are from the dynamical inversion, as described in section 2.4.

compares them to that of the MODIS grid mean LAI at each of the three sites. The gray areas about the MODIS LAIs indicate the variance of the grid means. At Walker Branch, we also include the LAIs derived from field measured fractional transmittance of PAR and litter basket collections at a location within 1-mile distance and with the same vegetation coverage in the Oak Ridge Free-Air CO2 Enrichment (FACE) experiment [*Norby et al.*, 2003].

[20] LAI seasonal cycles from the two types of inversions and from the MODIS derivation all capture the strong seasonality of deciduous forests with very low values in winter and large values in summer although the MODIS LAIs commonly show a broader period of peak LAI values than the dynamical and direct inversions do. Overall, the dynamical inversion is able to provide a smooth seasonal cycle of LAIs with reasonable values for each of the three testing sites whether or not the forcing data have been smoothed. In contrast, the seasonal cycles from the direct

inversion or that derived from MODIS observations contain a significant amount of fluctuations throughout the growing season. At Walker Branch, the dynamical inversion agrees with the field measurement well in the first half of the growing season, but show significantly lower values than MODIS LAIs between day 100 and 120. The agreement between the dynamical inversion and the MODIS LAIs is good in the second half of growing season. If we exclude the two high LAI value points in early growing season, the overall agreement between the MODIS and the dynamical inversion becomes much better, indicating that the high values may have been overestimations. The high MODIS LAI values in the early growing season at Harvard Forest may also due in part to overestimation given that the field phenology measurement shows that its LAI peaks on average between day 160 and 200 across all forest species (J. O'Keefe, unpublished data, 2004), while the MODIS LAI peaks on about day 140, substantially earlier than the field observations.

[21] Figure 4 compares the model simulated albedos based on LAIs from either dynamical inversion or from direct inversion, with the MODIS albedos. The albedo seasonal cycles from both dynamical and direct inversions agree well with that of the MODIS albedos in both the visible band and the near infrared band at all three testing sites except that the dynamical inversion is smoother and the direct inversions tend to match the point-to-point fluctuation of the MODIS albedos better, i.e., exactly what the dynamical inversion formulated to avoid.

[22] The adjusted parameters ("derived" in Table 2) via the dynamical inversion reflect the optimization of the cost function as defined in equation (3). Some of them have
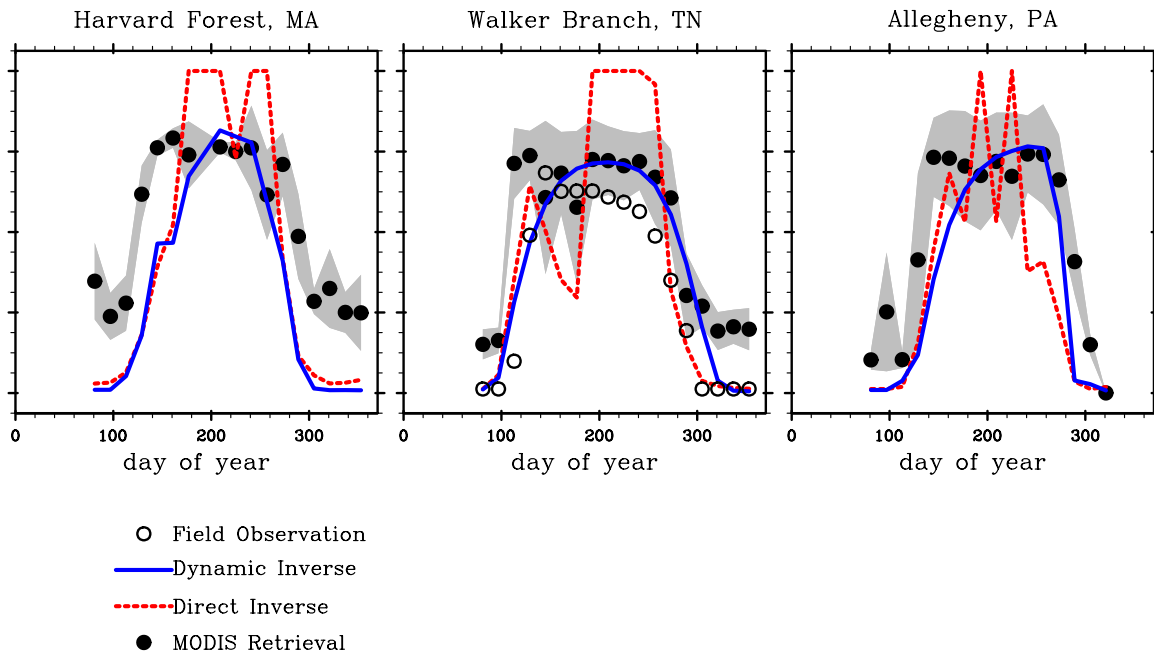

Figure 3. Comparison of the leaf area index (LAI) seasonal cycle based on direct inversion (dashed lines), dynamical inversion (solid lines), and Moderate-Resolution Imaging Spectrometer (MODIS) LAI product (solid circles), respectively. Field-based LAI observations (open circles) from the Free-Air CO$_2$ Enrichment experiment at a neighboring location [*Norby et al.*, 2003] of the Walker Branch are also shown for comparison. The shaded area depicts the standard deviations of the MODIS LAI computed from variance of the 49 pixel-level values for each site.
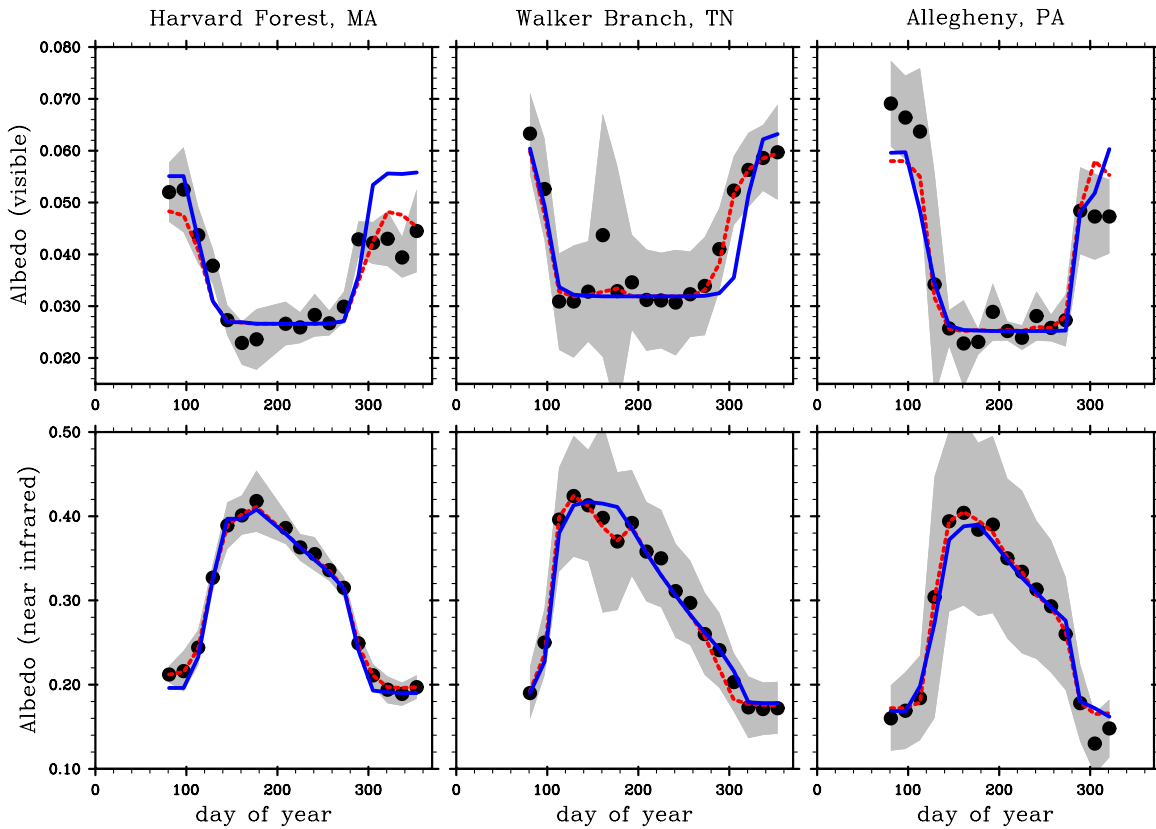
Figure 4. Same as Figure 3, but for comparisons of the surface albedos for diffuse radiation in the visible band, i.e., MODIS band 1 (top) and near-infrared band, i.e., MODIS band 2 (bottom), respectively. The white-sky surface albedos are derived from the MODIS collection 4 16-day, 1-km surface product of Bidirectional Reflectance Distribution Function (BRDF)/Albedo Model parameters at Harvard (left), Walker Branch (middle), and Allegheny (right). Each site has a 7 × 7 km patch or 49 pixels. The albedo values (circles) are the means of the pixel values, excluding missing points. The shaded area indicates the standard deviation computed from the variance of the pixel values.

reached the boundary of their given value ranges (e.g., parameter L_0 for Harvard and Walker Branch) indicating they are largely constrained by the provided value ranges. Evidently, reasonable predefined value ranges of the adjusted model parameters are also essential for the optimization of the model.

5. Discussion and Conclusions

[23] We have combined satellite-observed reflectances with a dynamical leaf model in a statistically optimal manner for the derivation of the LAI products that are consistent with a representation of the intrinsic dynamics of the vegetation. The results from three testing sites have shown that the proposed approach is able to produce reasonable LAI seasonal cycles without the erratic fluctuations in time that are typical of directly retrieved satellite LAI products.

[24] Direct inversion schemes that do not include any correlation between observations at different times and so may result in significantly sharp fluctuations in the obtained LAI in contrast with the dynamical inversion (i.e., as shown in Figure 3). Incorporation of a priori knowledge into the definition of the cost function (e.g., through the varying of the weighing matrix as was done by *Pinty et al.* [2007]) can

in theory reduce the amplitude of the erratic fluctuations. However, without the constraint of a dynamical leaf model, such treatments may be somewhat more arbitrary than is the dynamical inversion presented in this article, and thus, without further operations, may not provide LAI data products with the necessary smoothness for climate and carbon models.

[25] The implementation details shown in this article are for relatively ideal landscape conditions, i.e., homogenous closed-canopy vegetation cover, and dominant temperature-driven seasonal leaf dynamics. Consideration of soil moisture stress would also be necessary for tropical and semiarid regions. More sophisticated vegetation dynamic models need to be used to address the effects of other nonclimatic factors on the leaf dynamics such as land use/land cover change, logging, wildfire etc.. Its application for highly heterogeneous landscapes such as those with mixed vegetation types or with significant amount of bare soils or snow coverage would requires modification of the current statistical estimation of site level MODIS albedo with its uncertainty treating all the pixels with equal weight, i.e., different weights should be applied to pixels with different vegetation cover types. Realistic canopy 3-D radiation models with enough simplicity for economical implementation in a climate model would also be needed for heterogeneous

landscapes because the two-stream approximation of the canopy radiative transferring produce very large uncertainties in such cases. However, the general concept of this article would still apply under these conditions.

[26] The proposed data assimilation framework provides a mathematical constraint for numerical models to achieve optimal model-data agreement. Its successful applications still relay largely on an understanding of the data and of the physical properties of the models used. Such knowledge is necessary for providing the physical constraints to the modeling system. Therefore, targeted measurement of key model properties such as sensitive model parameters should be useful to the application of the proposed approaches.

[27] In conclusion, we proposed here a new approach to advance the retrieval of LAI from satellite-observed surface reflectances. The approach reduces the erratic temporal fluctuations commonly present in LAI products. It provides LAI products that are consistent with our understanding of seasonal dynamics of LAI and should satisfy the requirement by climate and carbon models. Further improvement can be achieved with enhanced understanding of the data to be used and the physical properties of the dynamical model.

References

Bicheron, P., and M. Leroy (1999), A method of biophysical parameter retrieval at global scale by inversion of vegetation reflectance model, *Remote Sens. Environ.*, *67*, 251–266, doi:10.1016/S0034-4257(98)00083-2.

Byrd, R. H., P. Lu, and J. Nocedal (1995), A limited memory algorithm for bound constrained optimization, *SIAM J. Sci. Stat. Comput.*, *16*(5), 1190–1208, doi:10.1137/0916069.

Chen, J. M., et al. (2002), Derivation and validation of Canada-wide coarse-resolution leaf area index maps using high-resolution satellite imagery and ground measurements, *Remote Sens. Environ.*, *80*, 165–184, doi:10.1016/S0034-4257(01)00300-5.

Chen, J. M., F. Deng, and M. Chen (2006), Locally adjusted cubic-spline capping for reconstructing seasonal trajectories of a satellite-derived surface parameter, *IEEE Trans. Geosci. Remote Sens.*, *44*(8), 2230–2238, doi:10.1109/TGRS.2006.872084.

Deng, F., J. M. Chen, S. Plummer, M. Chen, and J. Pisek (2006), Algorithm for global leaf area index retrieval using satellite imagery, *IEEE Trans. Geosci. Remote Sens.*, *44*(8), 2219–2229, doi:10.1109/TGRS.2006.872100.

Dickinson, R. E. (1983), Land surface processes and climate-surface albedos and energy balance, *Adv. Geophys.*, *25*, 305–353.

Dickinson, R. E., Y. Tian, Q. Liu, and L. Zhou (2008), Dynamics of leaf area for climate and weather models, *J. Geophys. Res.*, *113*, D16115, doi:10.1029/2007JD008934.

Hascoët, L., and V. Pascual (2004), *TAPENADE 2.1 User's Guide*, INRIA, Sophia-Antipolis, France.

Knyazikhin, Y., J. V. Martonchik, R. B. Myneni, D. J. Diner, and S. W. Running (1998a), Synergistic algorithm for estimating vegetation canopy leaf area index and fraction of absorbed photosynthetically active radiation from MODIS and MISR data, *J. Geophys. Res.*, *103*, 32,257–32,275, doi:10.1029/98JD02462.

Knyazikhin, Y., J. V. Martonchik, D. J. Diner, R. B. Myneni, M. M. Verstraete, B. Pinty, and N. Gobron (1998b), Estimation of vegetation canopy leaf area index and fraction of absorbed photosynthetically active radiation from atmosphere-corrected MISR data, *J. Geophys. Res.*, *103*, 32,239–32,256, doi:10.1029/98JD02461.

Lotsch, A., Y. Tian, M. A. Friedl, and R. B. Myneni (2003), Land cover mapping in support of LAI and FPAR retrievals from EOS-MODIS and MISR: Classification methods and sensitivities to errors, *Int. J. Remote Sens.*, *24*(10), 1997–2016, doi:10.1080/01431160210154858.

Myneni, R. B., Y. Knyazikhin, J. L. Privette, and J. Glassy (2002), Global products of vegetation leaf area and fraction absorbed PAR from year one of MODIS data, *Remote Sens. Environ.*, *83*, 214–231, doi:10.1016/S0034-4257(02)00074-3.

Norby, R. J., J. D. Sholtis, C. A. Gunderson, and S. S. Jawdy (2003), Leaf dynamics of a deciduous forest canopy: No response to elevated CO_2, *Oecologia*, *136*, 574–584, doi:10.1007/s00442-003-1296-2.

Oleson, K. W. et al. (2004), Technical description of the Community Land Model (CLM), *Tech. Note NCAR/TN-461+STR*, Natl. Cent. for Atmos. Res., Boulder, Colo.

Pinty, B., T. Lavergne, R. E. Dickinson, J.-L. Widlowski, N. Gobron, and M. M. Verstraete (2006), Simplifying the interaction of land surfaces with radiation for relating remote sensing products to climate models, *J. Geophys. Res.*, *111*, D02116, doi:10.1029/2005JD005952.

Pinty, B., T. Lavergne, M. Voßbeck, T. Kaminski, O. Aussedat, R. Giering, N. Gobron, M. Taberner, M. M. Verstraete, and J.-L. Widlowski (2007), Retrieving surface parameters for climate models from Moderate Resolution Imaging Spectroradiometer (MODIS)–Multiangle Imaging Spectroradiometer (MISR) albedo products, *J. Geophys. Res.*, *112*, D10116, doi:10.1029/2006JD008105.

Roerink, G. J., M. Menenti, and W. Verhoef (2000), Reconstructing cloud free NDVI composites using Fourier analysis of time series, *Int. J. Remote Sens.*, *21*(9), 1911–1917, doi:10.1080/014311600209814.

Schaaf, C. B., et al. (2002), First operational BRDF, albedo, and nadir reflectance products from MODIS, *Remote Sens. Environ.*, *83*, 135–148, doi:10.1016/S0034-4257(02)00091-3.

Sellers, P. J., Y. Mintz, Y. C. Sud, and A. Dalcher (1986), A simple biospheric model (Sib) for use with general circulation models, *J. Atmos. Sci.*, *43*, 505–531, doi:10.1175/1520-0469(1986)043<0505:ASBMFU>2.0.CO;2.

Tian, Y., R. E. Dickinson, L. Zhou, and M. Shaikh (2004), Impact of new land boundary conditions from Moderate Resolution Imaging Spectroradiometer (MODIS) data on the climatology of land surface variables, *J. Geophys. Res.*, *109*, D20115, doi:10.1029/2003JD004499.

Yang, W. Z., et al. (2006), MODIS leaf area index products: From validation to algorithm improvement, *IEEE Trans. Geosci. Remote Sens.*, *44*(7), 1885–1898, doi:10.1109/TGRS.2006.871215.

Zarco-Tejada, P. J., C. A. Rueda, and S. J. Ustin (2003), Water content estimation in vegetation with MODIS reflectance data and model inversion methods, *Remote Sens. Environ.*, *85*, 109–125, doi:10.1016/S0034-4257(02)00197-9.

Zeng, X., M. Shaikh, Y. Dai, and R. E. Dickinson (2002), Coupling of the Common Land Model to the NCAR Community Climate Model, *J. Clim.*, *15*, 1832–1854, doi:10.1175/1520-0442(2002)015<1832:COTCLM>2.0.CO;2.

Zhu, C., R. H. Byrd, and J. Nocedal (1997), L-BFGS-B: Algorithm 778: L-BFGS-B, FORTRAN routines for large scale bound constrained optimization, *Trans. Math. Software*, *23*(4), 550–560, doi:10.1145/279232.279236.

————————————

R. E. Dickinson, Q. Liu, and L. Zhou, School of Earth and Atmospheric Sciences, Georgia Institute of Technology, 311 Ferst Drive, Atlanta, GA 30332-0340, USA. (ql11@mail.gatech.edu)

L. Gu and W. M. Post, Environmental Sciences Division, Oak Ridge National Laboratory, Oak Ridge, TN 37831, USA.

Y. Tian, Center for Satellite Applications and Research, IMSG, NOAA/NESDIS, Camp Springs, MD 20746, USA.